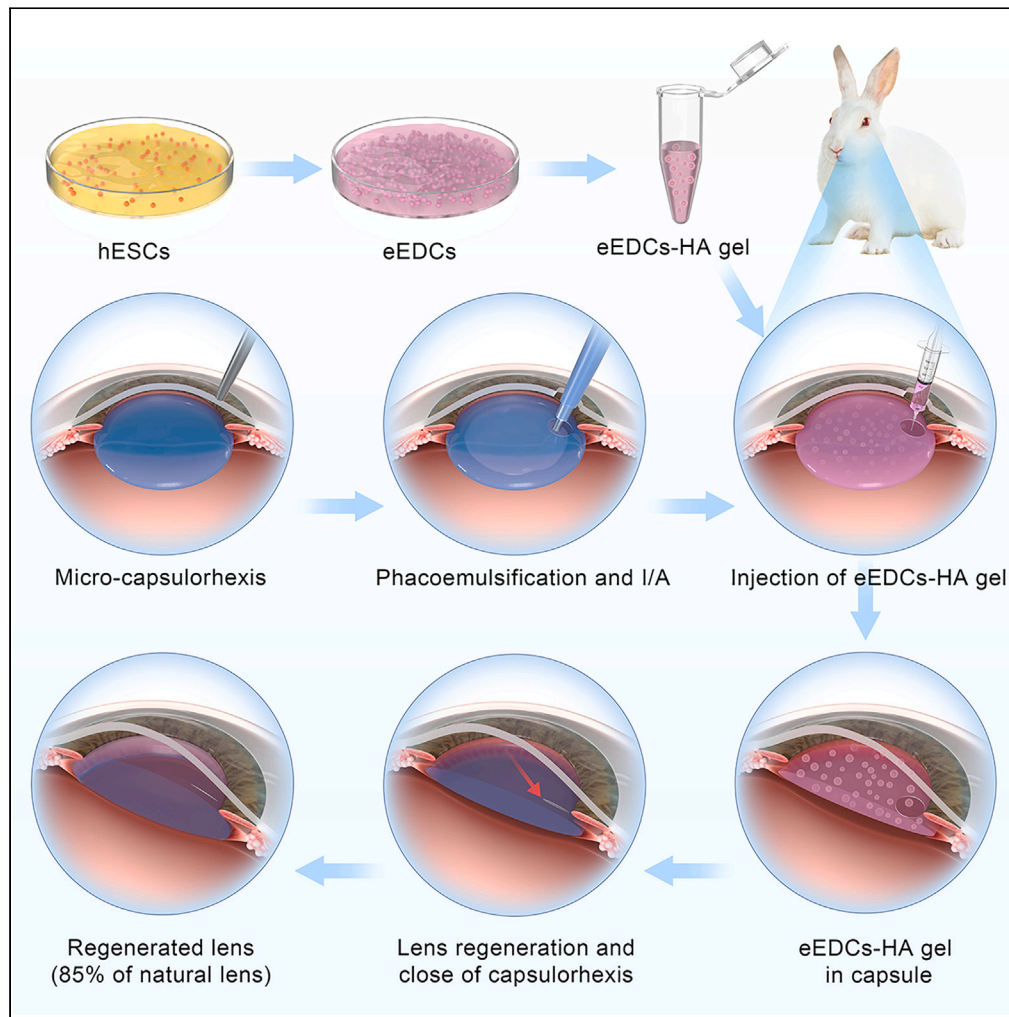


Article

# Lens regeneration *in situ* using hESCs-derived cells—similar to natural lens



Xinyi Chen, Hanle Wang, Hui Chen, ..., Peike Hu, Qiuli Fu, Ke Yao

2313009@zju.edu.cn (Q.F.)  
xlren@zju.edu.cn (K.Y.)

**Highlights**

Lens was regenerated *in situ* using hESCs-derived cells—similar to natural lens

The regenerated lens is the most transparent, thickest one

The participation of the Wnt/PCP pathway in lens regeneration was verified

This provides a new therapeutic strategy and development direction for cataracts

Chen et al., iScience 26, 106921  
June 16, 2023 © 2023 The Author(s).  
<https://doi.org/10.1016/j.isci.2023.106921>



## Article

Lens regeneration *in situ* using hESCs-derived cells —similar to natural lens

Xinyi Chen,<sup>1,3</sup> Hanle Wang,<sup>1,3</sup> Hui Chen,<sup>1,2,3</sup> Ling Ren,<sup>1</sup> Wei Wang,<sup>1</sup> Jingjie Xu,<sup>1</sup> Chenqi Luo,<sup>1</sup> Peike Hu,<sup>1</sup> Qiuli Fu,<sup>1,\*</sup> and Ke Yao<sup>1,4,\*</sup>

## SUMMARY

**Lens itself has limited regeneration functionality, thus we aimed to create regenerated lens with biological function to treat cataracts rather than the intraocular lens used in cataract surgery. We induced exogenous human embryonic stem cells to directionally differentiate into lens fate like cells *in vitro*, mixed these cells with hyaluronate, and then implanted the mixture into lens capsule to regenerate *in vivo*. We successfully achieved near-complete lens regeneration, and the thickness of the regenerated lens reached 85% of the contralateral eye, showing the characteristics of biconvex shape, transparency, and a thickness and diopter close to that of natural lenses. Meanwhile, the participation of Wnt/PCP pathway in lens regeneration was verified. The regenerated lens in this study was the most transparent, thickest, and most similar to the original natural lens that has thus far been reported. Overall, these findings offer a new therapeutic strategy for cataracts and other lens diseases.**

## INTRODUCTION

Cataract is one of the most significant blinding diseases in the world, affecting approximately 65.2 million people.<sup>1,2</sup> According to the World Health Organization, cataract is the world's leading eye disease causing blindness, with approximately 51% of blindness related to cataract. In addition to the removal of the opaque lens by surgery, researchers have sought to create a replacement lens via stem-cell regeneration with a biological function similar to the natural lens; this would allow for the exploration of new cataract treatment methods.<sup>3</sup> The lenses of some species have regeneration ability, but the degree and mechanism of regeneration vary.<sup>4–6</sup> Lenses can be completely regenerated in lower vertebrates after lens injury or extraction. In rabbit eyes, regenerated lens tissue partly appears around the capsule 3–5 weeks after lens extraction.<sup>7</sup> Meanwhile, it has generally been found in clinical work that some transparent regenerated lens-like structures are formed around the lens capsule in children's eyes shortly after cataract surgery.<sup>8</sup> However, it is worth noting that the lens regeneration ability of higher mammals is relatively weak,<sup>9</sup> and there are significant requirements for the regeneration microenvironment that are especially dependent on the existence and condition of the lens capsule. In 2016, a research team<sup>8</sup> successfully utilized lens epithelial cells (LECs) under the anterior capsule and used their partial self-renewal and differentiation characteristics as endogenous stem cells to achieve the partial regeneration of lens tissue in New Zealand rabbits, long-tailed macaques, and children with congenital cataracts. This provides a new paradigm and possibility for the application of endogenous stem cells in tissue regeneration.<sup>10</sup> Partial lens regeneration is achieved through the proliferation and migration of LECs remaining under the capsule.<sup>11</sup> Although partial lens regeneration was achieved in the study by Lin et al., lens regeneration in mammals is not simply a repetition of lens development. Disordered proliferation, migration, and the transformation of residual LECs affect the transparency of regenerated lenses. The figures in that study showed that the lens regenerated by the endogenous stem cells was opaque, and there remained a significant disparity between the regenerated lens and a natural lens in terms of shape, thickness, structure, optical property, etc.<sup>12</sup> In addition, this form of LEC-derived lens regeneration is not suitable for patients with gene-related congenital cataracts. In such cases, the patient's own LECs still carry the related mutations or genetic sites, and thus the regenerated lens may appear with cataracts similar to the primary disease. Therefore, the application of LECs with stem cell characteristics is constricted, the proliferation ability of LECs is limited, and the thickness, development characteristics, transparency, and optical properties of LECs are difficult to guarantee. Thus, whether cells derived from exogenous stem cells can be supplemented or replaced to achieve the purpose of complete lens regeneration is key to addressing this problem.

<sup>1</sup>Eye Center of the Second Affiliated Hospital, Zhejiang University School of Medicine, 88 Jiefang Road, Hangzhou 310009, China

<sup>2</sup>Eye Hospital and School of Ophthalmology and Optometry, Wenzhou Medical University, Wenzhou, China

<sup>3</sup>These authors contributed equally

<sup>4</sup>Lead contact

\*Correspondence: 2313009@zju.edu.cn (Q.F.), xiren@zju.edu.cn (K.Y.)

<https://doi.org/10.1016/j.isci.2023.106921>



Furthermore, embryonic stem cells (ESCs) and induced pluripotent stem cells (iPSCs) can be successfully induced in lens progenitor cells (LPCs) and the lentoid body (LB) *in vitro*. First, Ooto et al.<sup>13</sup> induced to differentiate to lens-specific marker positive tissue mass by co-culture of ESCs and PA6 cells, but its application was limited because of its co-culture induction mode. After that, Yang et al.<sup>14</sup> successfully induced ESCs for differentiation into LPCs and the LB *in vitro* using a three-step method combined with specific growth factors; this caused the *in-vitro* induction of the lens to eliminate the co-culture mode and broadened the idea for lens regeneration *in vitro*. However, the function of a lens lies in its transparency and refraction. Although the LB obtained using the three-step method expresses mature lens markers including  $\alpha$ A-,  $\alpha$ B-,  $\beta$ -,  $\gamma$ -crystalline, and MIP, it cannot reproduce the optical function of a lens, so its application is greatly limited. Our research team has successfully used iPSCs from human urine to induce iPSCs in the LB through the original "fried egg" method; this represents the first LB with optical properties.<sup>15</sup> The "fried egg" method is the most mature method for constructing the LB *in vitro* that has been reported thus far and has obtained a Chinese invention patent (ZL 2015 1 0617265.0). On the basis of the following three-step method, the differentiated cells around the cell cluster were cut and mechanically separated after six days of stimulation, with noggin factor used during the first stage, which is the LPCs. The peripheral epithelial-like cells were selected and implanted into the culture medium of bFGF-BMP7 in the second stage and then stimulated with bFGF-Wnt3a in the third stage. When the differentiation of D25 was completed, a three-dimensional, transparent, and refractive LB with a diameter of 3 mm was obtained, which expressed mature lens markers. Although the method used for the *in-vitro* mechanical separation of the LPCs for lens regeneration has been well established, transplantation *in vivo* after LB regeneration *in vitro* remains difficult to realize. Because there are no blood vessels, muscles, ligaments, etc., in lenses, they easily become opaque with changes in the *in-vivo* microenvironment. At the same time, the size, shape, thickness, and other properties of LBs regenerated *in vitro* are still vastly different from those of natural lenses. Therefore, the *in-situ* regeneration of lenses that can be entirely completed in the capsule *in vivo* continues to be the ultimate goal.

The rapid development of stem cell technology has provided new treatment ideas and hope for a variety of difficult-to-treat diseases. Therefore, we hope that on the basis of our team's experience inducing iPSCs to differentiate LPCs *in vitro*, the technology of the directional differentiation of stem cells can be used to induce exogenous hESCs to be directionally differentiated into early ESC-derived differentiated cells (eEDCs) *in vitro*. This process occurs a very early stage of development, which are then regenerated *in vivo* to form a structure similar to a normal natural lens. This treatment can avoid the many disadvantages of intraocular lenses, maintain the physiological and functional balance of patients' eyes, as well as overcome the problems of the low transparency, insufficient functionality, and limited application of endogenous LECs. Ultimately, a regenerated lens with high transparency, appropriate thickness, and refractive and adjustment ability close to a natural lens was obtained, which may represent a new era in the prevention and treatment of cataracts.

## RESULTS

### Morphology of regenerated lens

After the implantation of the eEDCs-HA gel compound into the rabbit's eye, the lens was successfully regenerated, and the thickness of the regenerated lens reached 85% of the contralateral eye (Figure 1). The lens regenerated from eEDCs was found to show the characteristics of biconvex shape and high transparency. Compared to the lens regenerated from endogenous LECs,<sup>8</sup> which reached a stable regeneration outcome at 7 W after surgery, the lens regenerated from eEDCs showed a different regeneration process, involving continued thickening after 7 W and exhibiting the characteristics of longer continuous regeneration time (Figure 2; 3).

Within 3 W after the operation, the lens regeneration was slowed such that it could not be observed. A slit lamp showed that the anterior and posterior capsules were close to each other, and the space between the anterior and posterior capsule was not significantly thickened (Figures 2Aa and 2Ca). From 4 W after the operation, the separation of the anterior and posterior capsules peripherally around the capsules was observed, and the distribution of the contents in the capsule was obvious. The first peak stage of lens regeneration was 4–6 W, in which the regeneration formation changed from peripherally surrounding the capsule to a biconvex shape (Figures 2Ab, 2Ac, 2Cb, and 2Cc). At this stage, the regeneration speed in the center of the capsule was significantly higher than that in the periphery. After 6 W, the regenerated lens began to gradually thicken, maintaining the normal convex lens shape, and grow slowly (Figures 2Ad

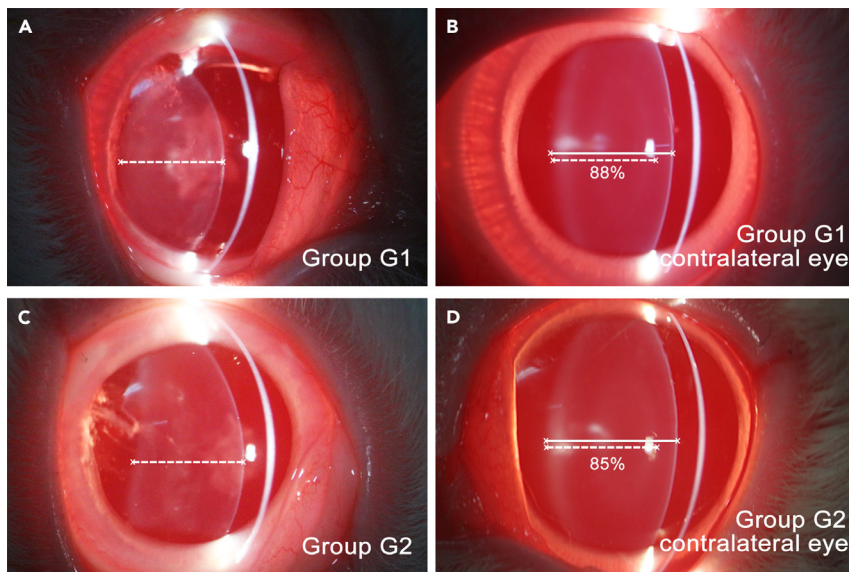


**Figure 1. Comparison of the regenerated lens and contralateral eye of G1 and G2 rabbits at 80W**

(A) G1 regenerated lens.

(B) G1 contralateral eye; the thickness of the regenerated lens reached 88% of the contralateral eye.

(C) G2 regenerated lens.

(D) G2 contralateral eye; the thickness of the regenerated lens reached 85% of the contralateral eye. G1, No. 1 rabbit of Group G; G2, No. 2 rabbit of Group G.

and 2Cd). From 12 to 20 W, the second peak of lens regeneration occurred, and the thickness of the regenerated lens increased faster than that during 6–12 W (Figures 2A e–g and 2C e–g). After 20 W, the lens began to regenerate slowly (Figures 2Ah–k and 2Ch–k). Until 54 W, the lens regeneration process tended to be stable, and the thickness change was not obvious (Figures 2Ak, l and 2Ck, l). The ratio curve of the regenerated lens thickness to the contralateral lens thickness at different time points is shown in Figures 2B and 2D.

As shown in these retro-illumination figures, the regenerated lens grew from the periphery at the initial stage before 4 W (Figures 3Aa, 3Ab, 3Ba, and 3Bb) and gradually filled the anterior and posterior capsules to the center at about 6 W (Figures 3Ac and 3Bc). The regenerated lens showed uneven growth in the middle stage from 8 to 20 W (Figures 3Ad–Ag; 3B d–g), gradual and orderly growth at the later stage of 25 W (Figures 3Ah and 3Bh), and stable and transparent growth after 40 W (Figures 3Ai–l and 3Bil). In the process of lens regeneration, we also observed interesting phenomena. The position of the capsulorhexis after surgery was not obvious, but there was a replaced fold near the anterior capsulorhexis. According to observations, we found that the micro-capsulorhexis may be partially or fully closed (Figure 3, red arrow). At the same time, in the follow-up observations of regeneration, the position of the capsulorhexis area also showed the existence of the regenerated lens, rather than showing no regeneration as in the previous study.<sup>8</sup> Another notable phenomenon that occurred at 6–15 W after the operation was observed: the beaded opacity around the regenerated lens was similar to that of the posterior capsular opacification (PCO) (Figures 3Ae, m; 3Bf, m), which reached the maximum (Figures 3Ag, n; 3Bg, n). Then, the beaded changes began to decrease (Figures 3Ag, o; 3Bh, o) and later completely disappeared (Figures 3Ai, p; 3Bi, p).

### Clinical evaluation of regenerated lens

Pentacam and UBM were considered for use for the *in-vivo* clinical evaluation of the regenerated lens after operation. 12 W was the last normal checkpoint at which the Pentacam could be used to measure the thickness of lens, and the regenerated lens was about 3-mm thick (Figure 4B). Subsequently, when the lens was checked at 54 W, the results showed a biconvex lens shape, and the arch curvature of the front surface of the regenerated lens was similar to the contralateral control eye (Figures 4C and 4D). Furthermore, and no obvious opacity area was found during either examination.

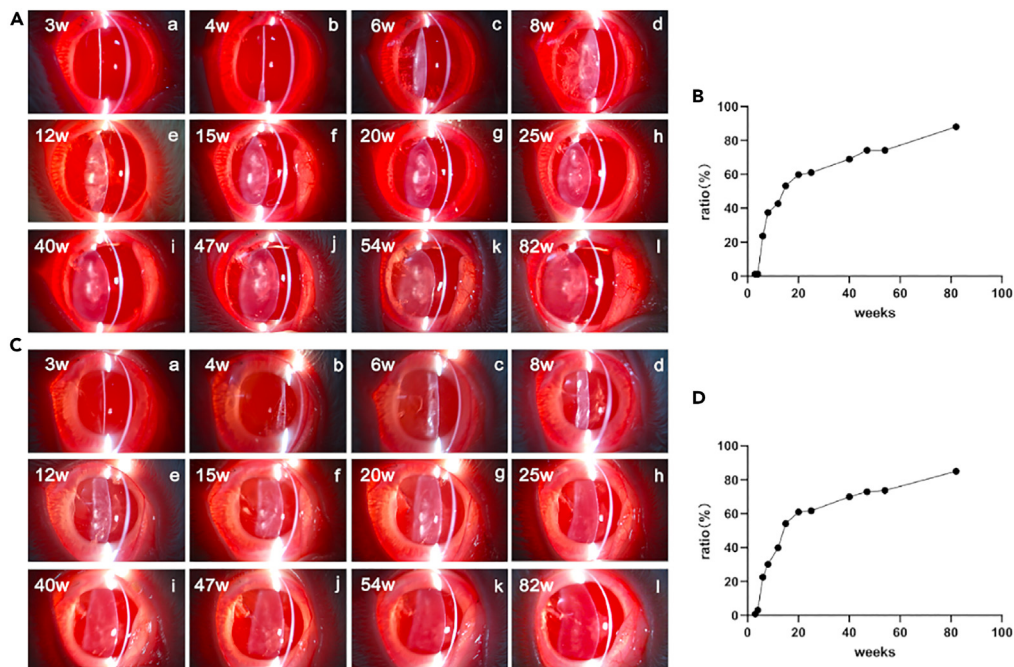


**Figure 2. Regeneration process from 3 W to 82 W in Groups G1 and G2**

(A and C) Slit lamp figure of G1 and G2: (a) Anterior and posterior capsules were close to each other. (b and c) First peak stage of lens regeneration. (d) Regenerated lens thickened gradually, maintained the normal convex lens shape, and grew slowly. (e–g) Second peak of lens regeneration occurred. (h–k) Lens began to regenerate slowly. (i) State of regenerated lens was stable and there was a very slow increase in thickness. (B, D) Ratio curve of G1 and G2 regenerated lens thickness to contralateral lens thickness at different time points.

In addition, at 20 W, the rabbits in Group F were euthanized, and the lenses were harvested. The thickness and magnification of the lenses were immediately measured. The thickness of the central lenses was about 5 mm (thickness at 12 W: 3.2 mm). The lenses were observed as transparent under the microscope, with only a small amount of opacity, and the amplification efficiency was high (Figure 4A).

Meanwhile, during the follow-up, the operation eyes and the contralateral eyes were examined by retinoscopy to obtain the refractive diopters. The results are shown in Figure 4E. At 82 W, the operated eyes were  $+5.17 \pm 0.29D$ , and similarly, the contralateral eyes were  $+3.08 \pm 0.52D$ .

In short, near-complete lens regeneration from eEDCs was realized, and the regenerated lens showed the characteristics of biconvex shape, high transparency, and a thickness and diopter closer to those of a natural lens than those of the partial lens regenerated from endogenous LECs in a previous study.<sup>8</sup>

### Safety evaluation

To simply and conveniently detect the survival and vitality of the cells mixed with the carrier materials, we carried out *in-vitro* simulation tests. During this testing, 0.2 mL of the eEDCs-HA gel compound was cultured in the culture dish. After one day, the gel compound became thinner, and the cells almost completely adhered. After three days, no colloidal substance remained. Furthermore, there was no significant difference in cell death rate and cell morphology between the eEDCs-HA gel compound culture and control culture at D1, D3, and D5 (Figure S2). Hence, the survival and vitality of the cells was not affected by the carrier materials.

We also tested the IOP after surgery, and the results are shown in Figure 4F. The IOP of the operated eye increased slightly on the first day after operation, and decreased thereafter. The IOP of the operated eye at

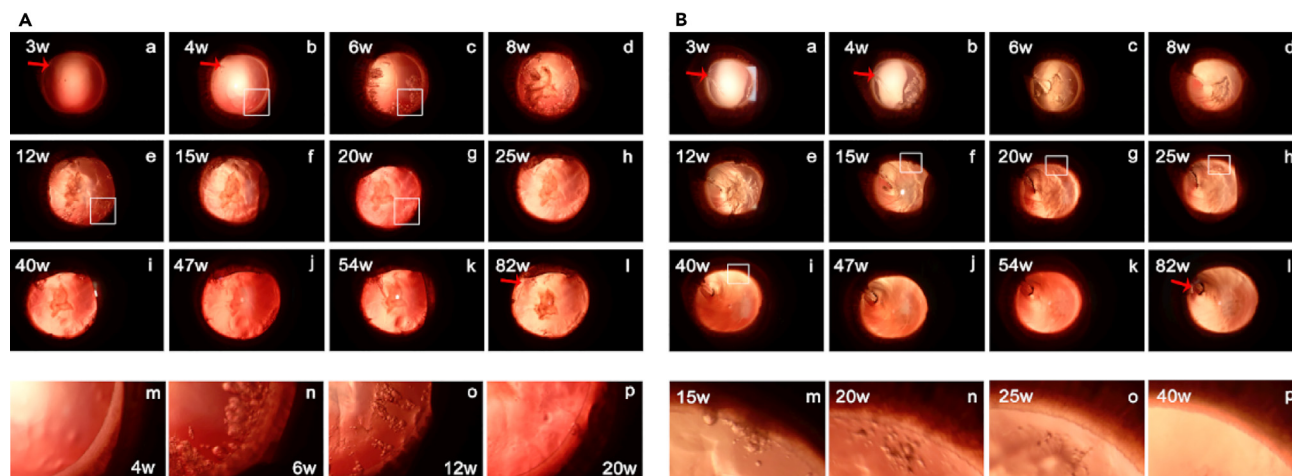


**Figure 3. Regeneration process from 3 W to 80 W in Groups G1 and G2 by slit lamp retroillumination**

(A) G1. (B) G2: (a, b) Regenerated lens grew from the periphery; (red arrow) capsulorhexis was partially closed. (c) Regenerated lens gradually filled the anterior and posterior capsules to the center. (d–g) Uneven growth of regenerated lens. (h) Lens regenerated gradually and orderly. (i–l) Regenerated lens was stable and transparent; (red arrow) capsulorhexis area also showed the existence of regenerated lens. A: (m–p) Enlarged part of box areas at b, c, e, and g. B: (m–p) Enlarged part of box areas at f–i. (m) Beaded opacity around the regenerated lens was similar to that of PCO. (n) Beaded opacity reached the maximum. (o) Beaded changes began to decrease. (p) Beaded opacity disappeared completely.

D1 was higher than at D3, D7, D14, and D28 ( $p = 0.043$ ,  $p = 0.012$ ,  $p = 0.01$ ,  $p = 0.019$ ), whereas there was no significant difference between D3, D7, D14, and D28 ( $p > 0.05$ ). On D1, the IOP of the operated eye was significantly higher than that of the contralateral eye ( $p = 0.013$ ). The intraocular pressure of the operated eye returned to the preoperative level of D3 after operation, and there was no significant difference compared to that of the contralateral eye (D3, D7, D14, D28,  $p > 0.05$ ). Therefore, the experimental method did not cause any damage to the trabecular meshwork of the rabbit eyes.

A tumorigenicity experiment in nude mice was conducted to verify the safety of the stem cell derivatives. NS, eEDCs, eEDCs with Matrigel, and ML-3 cell groups from top to bottom. No tumorigenicity was detected in the nude mice in the NS, eEDC, and eEDC with Matrigel groups. Only the positive control group of HCCML-3 cells group showed tumor tissue after 4 weeks' observation (Figure S4). Our subcutaneous tumorigenesis experiment in nude mice indicated that the eEDCs had no significant tumorigenicity. Moreover, all rabbits from Groups A–F were subjected to general and basic eye examinations, and we confirmed that they were healthy before they were euthanized. Meanwhile, to verify the long-term effects of eEDCs on rabbits *in vivo*, we dissected a Group G rabbit that had been raised and observed for a significant time and carried out H&E staining on the main organ tissues, cornea, and retina. The results are shown in Figure S5, which demonstrates that the main organs of the rabbits with eEDC implantation had no tumor tissue proliferation, and the tissue structure was not affected. All of these demonstrated that eEDC implantation has good long-term safety.

### Expression of lens-specific markers in regenerated lens

We then examined the expression of FOXE3 (lens epithelial cell markers and specific early lens markers) and  $\alpha$ A- and  $\alpha$ B-crystallin (specific early lens markers and primary lens fiber cell markers), as well as  $\beta$ - and  $\gamma$ -crystallin (mature lens fiber cell markers) during the regeneration process. The regeneration tissue expressed the lens-specific markers, thus verifying the regenerated lens. Our results showed that the expression level of  $\alpha$ B-crystallin gradually increased as regeneration progressed, whereas  $\alpha$ A-,  $\beta$ -, and  $\gamma$ -crystallin first increased, peaked at 8 W (Figure 5), and then decreased. As well, the expression of these early and mature fiber cell markers showed a continuous regeneration process. Changes in FOXE3 were totally different from the other changes. FOXE3 was positive in all nucleated cells at 3 W, whether in the interior of the lens capsule, under the anterior capsule, or at the equator. Over time, at 6 W, only a small number of cells in the interior of the lens capsule were FOXE3-positive, whereas the nucleated cells under the anterior capsule and at the equator remained FOXE3-positive. At 8 W, the nucleated cells under the anterior capsule and at the equator were still FOXE3-positive; however, the results showed that the only

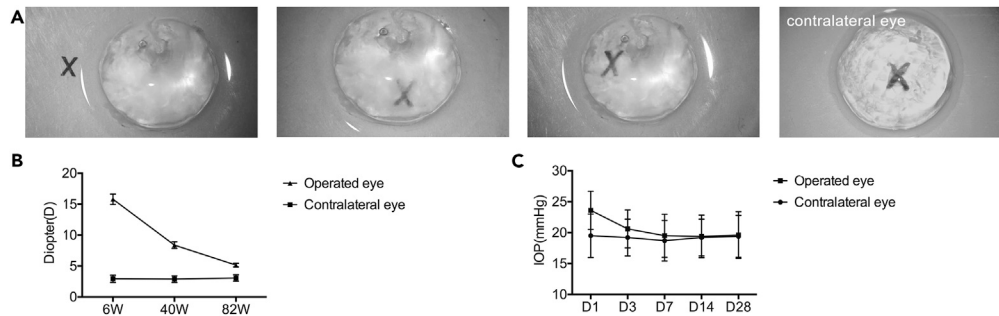


**Figure 4. Morphology and clinical evaluation of regenerated lens**

(A) Transparency and amplification efficiency of regenerated lens under the microscope.  
(B) Refractive diopter of the operation eyes and the contralateral eyes.  
(C) IOP of the operation eyes and the contralateral eyes.

nucleated cells under the anterior capsule, where the endogenous LECs are located, expressed FOXE3 at 12 W and 20 W, indicating possible changes in regeneration.

### Histopathology of regenerated lens

Histopathologic sections further revealed the progress of lens regeneration (Figure 6). The regenerated lens cells were arranged from those that were disorderly to those that appeared in a regular and close manner, and finally, to those that were similar to those of a natural lens. Before 8 W, a large number of nucleated cells was found in the central part of the capsule (Figure 6F), in addition to the monolayer LECs under the anterior capsule and at the equator. Furthermore, the density of the nucleated cells in the center of the capsule decreased with time. After 12 W, the nucleated cells could be seen under the anterior capsule and at the equator (Figure 6H). At the same time, the cells in the capsule were disorderly at 3 W (Figure 6B), whereas they were arranged closely and orderly at 6–8 W (Figures 6D and 6F) until 20 W (Figure 6L). At the same time, Figure 6 shows that the lens fibroblast cells were arranged in a regular and close manner, without obvious irregularity and confusion, and the arrangement was similar to that of a natural lens. The histological results were consistent with the results of the slit lamp examination *in vivo*.

### Cell resources of regenerated lens: Exogenous eEDCs

Because eEDCs were previously implanted into the rabbits' eye capsules, it was important to determine whether the regenerated lenses came from the endogenous rabbit LECs or the exogenous eEDCs. Therefore, we found a mouse monoclonal anti-GAPDH antibody (cell signaling) that only reacts with human cells. WB results showed that the regenerated lens, hESCs before implantation, and human lens (extracted from the fluid collection box of cataract surgery) were GAPDH-positive, whereas the contralateral control rabbit lens was GAPDH-negative (Figure 7B). It can thus be concluded that there were implanted cells in the regenerated lens. RNA-seq analysis also verified this result in another aspect (Figure 7C). After excluding gene matching with the rabbit reference genome (more than 80% of all reads), the ratio of residual reads mapped to the human reference genome showed significant differences between Groups F and H ( $6.967 \pm 0.8699$  vs.  $3.190 \pm 0.5882$ ,  $p = 0.023$ ). Figure 7A shows the positive expression of human-specific GAPDH in the regenerated lens and human lens by IHC and no expression in the contralateral control rabbit lens by IHC. In addition, the human-specific GAPDH positive cells were uniformly distributed within the regenerated lens and accumulated in the nucleated cells. After comparison, there were human-derived cells in the regenerated lens, and the proportion maintained stability and balance in the regenerated lens at different time points. Therefore, the regenerated lens was a product or part of a product of the exogenous eEDCs.

### Lens regeneration-related pathway: The non-canonical Wnt/PCP pathway

RNA-seq analysis and KEGG pathway enrichment analysis of the regenerated lens and contralateral eye (control group) indicated lens regeneration was associated with the Wnt signaling pathway and its related pathways, such as Ras, mTor, MAPK, and TGF- $\beta$  (Figures 8A). As c-Jun N-terminal kinase (JNK) and c-JUN play important roles in the non-canonical Wnt planar cell polarity (PCP) pathway, we further assessed the effects of JNK and c-JUN in the lens regeneration process. We found that JNK, phosphorylated JNK,

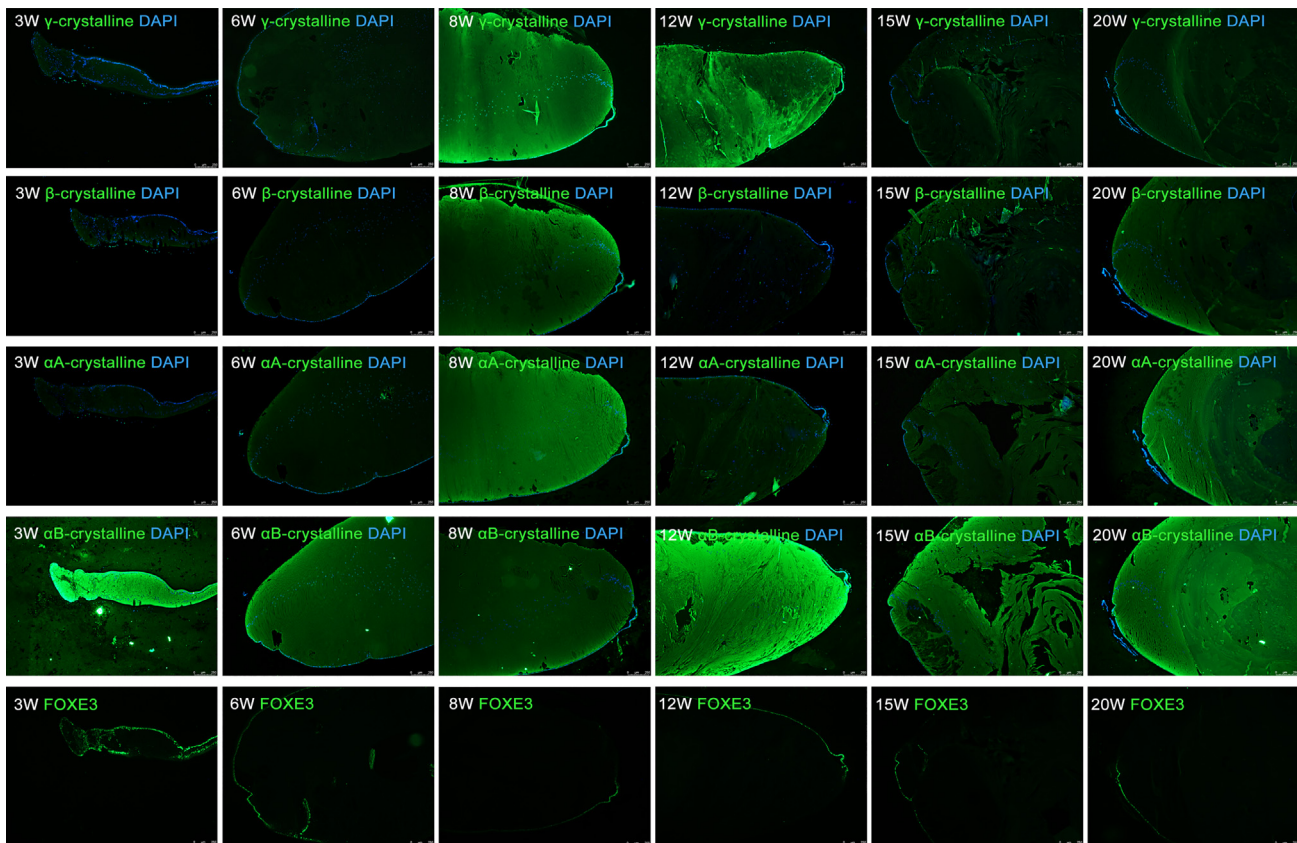


**Figure 5. Regenerated lens expressed specific early lens markers FOXE3 and  $\alpha$ A- and  $\alpha$ B-crystallin, as well as fiber cell markers  $\beta$ - and  $\gamma$ -crystallin during the regeneration process**

c-JUN, and phosphorylated c-JUN were highly increased during the early and middle stages of the lens regeneration process. Moreover, even in the late stage, the total amount of JNK and c-JUN protein was similar to that in the control group, whereas the phosphorylated JNK protein levels relative to the total JNK protein level and the phosphorylated c-JUN protein level relative to the total c-JUN protein and were significantly higher than in the control group (Figures 8B and 8C). This suggests that the stimulating non-canonical Wnt/PCP pathway participates in lens regeneration.

### Characteristics of resource cells

We detected the cell markers in the process of differentiation *in vitro* and found that with the extension of differentiation time, the expression of stem cell marker Nanog slowly decreased. There was also a significant decrease at D5, but Nanog remained positive. The epithelial cell marker E-cadherin was negative at D1 and D2, but there was little expression at D3 and obvious expression at D5. Therefore, we finally selected D5 cells for subsequent animal experiments (Figure 9).

### DISCUSSION

In this study, we used eEDCs implanted into the rabbit lens capsule to successfully regenerate the lens, and the thickness of the regenerated lens reached 85% of the contralateral eye. Compared to those in previous studies, the regenerated lens reported in this study is the most transparent, thickest, and most similar to the original natural lens in shape and refractive diopter, opening up a new direction for the treatment of cataract and other lens diseases.

As there has been little reference to the long-term process of *in-vivo* lens regeneration in previous studies, we conducted a large number of pre-experiments before formalizing the design of this study. Based on the results of previous studies, within 7 W of lens regeneration, we conducted a 10-W pre-experiment. The

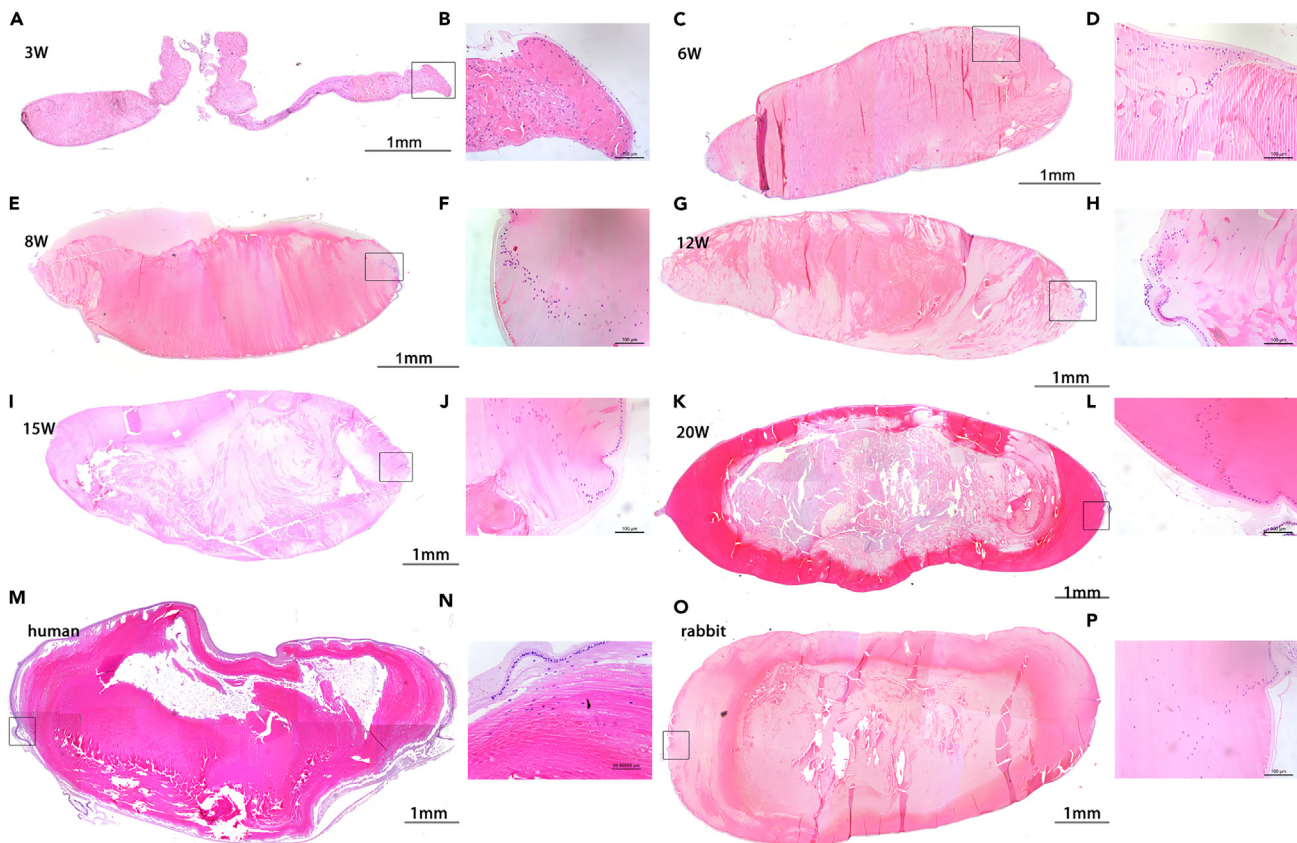


**Figure 6. Regenerated lens cell arrangements ranged from disorderly to regular and close, and finally to that similar to a natural lens**

(A and B) A large number of nucleated cells with disorderly organization in the central part of the capsule besides the monolayer LECs under the anterior capsule and at the equator.

(C and E) Density of nucleated cells in the center of the capsule decreased with time.

(D and F) Cells in the capsule had a close and orderly arrangement.

(G and H) Nucleated cells only under the anterior capsule and at the equator.

(I and J) Cells arranged more closely and orderly.

(K and L) Lens fibroblast cells arranged in a regular and close manner, similar to that of a natural lens.

(M and N) Human lens.

(O and P) Natural rabbit lens.

results of the pre-experiment were similar to those of the formal experiment. The growth rate of the regenerated lens reached the peak at 6 W and slowed significantly at 6–10 W. Therefore, in the formal experiment, we set the time point for the last collection of the lens for subsequent protein, RNA sequence, and histological observation to 20 W after surgery. At the same time, we reserved a long-term observation group (Group G) with which to obtain the *in-vivo* status of lens regeneration after 20 W. Furthermore, the results of this study showed that 10–20 W after surgery, not only was the lens regeneration ushered in during the second peak of regeneration speed, but it was still in a state of regeneration and thickening after 20 W—even one year after surgery. This represents a completely different process than the previous one, wherein endogenous LECs led lens regeneration.

At the same time, RNA sequencing and WB analysis showed that the regenerated lens was formed by the co-proliferation and differentiation of exogenous eEDCs and endogenous LECs. Moreover, this result constitutes also a completely new discovery, entirely overturning the hypothesis developed before our experimental design. We first designed the experiment believing that because endogenous LECs have limitations, we could replace the regeneration progress with a large number of exogenous eEDCs. We required the eEDCs showed characteristics that there is a part of the proliferation ability of stem cells to get sufficient cells for regeneration, and at the same time, similar ability as endogenous LECs and

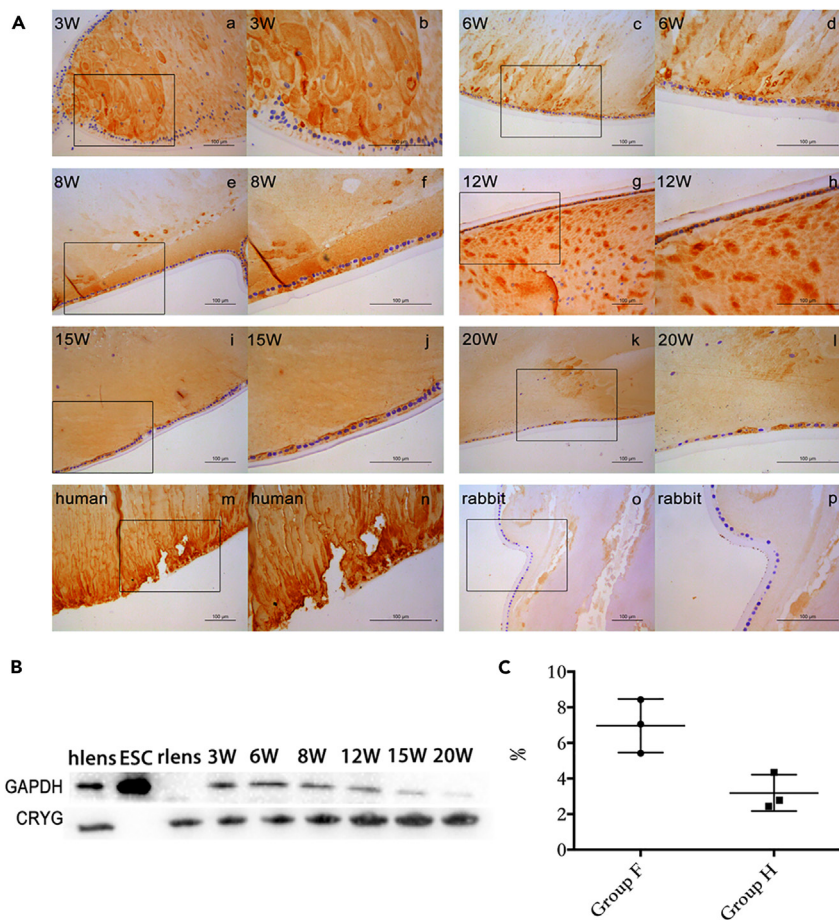


**Figure 7. Regenerated lens, hESCs before implantation, and human lens expressed human-specific GAPDH-positive by IHC and WB, while the contralateral control rabbit lens negative**

(A) (a–l) Expression of human-specific GAPDH in regenerated lens by IHC. (m, n) Expression of human-specific GAPDH in human lens by IHC. (o, p) No expression of human-specific GAPDH in contralateral control rabbit lens by IHC. (m, n) Expression of human-specific GAPDH in human lens by immunohistochemistry.

(B) Regenerated lens, hESCs before implantation, and human lens (extracted from the fluid collection box of cataract surgery) were human-specific GAPDH-positive, whereas the contralateral control rabbit lens was GAPDH-negative. h lens, human lens; r lens, contralateral control rabbit lens.

(C) After excluding gene matching with the rabbit reference genome (more than 80% of all reads), the ratio of residual reads mapped to the human reference genome was significantly higher in Group F than in Group H ( $p = 0.023$ ).

characteristics of epithelial cells begin to appear. Thus, from this point of view, the D5 cells were in line with our expectations. The expression of the stem cell marker Nanog showed a significant decrease at D5 but was still positive. E-cadherin and FOXE3 are widely accepted as lens epithelial cell markers, and the epithelial cell marker E-cadherin was negative at D1 and D2, but there was little expression at D3 and obvious expression at D5. We therefore selected the D5 cells that already strongly expressed epithelial cell identity. To the best of our ability, we sought to clean up the LECs under the anterior capsule and at the equator during the operation, so as to achieve a process of exogenous eEDC regeneration in the capsule environment. However, it was not expected that both endogenous and exogenous eEDCs would participate in the entire process and that the two cells would proliferate and differentiate together to regenerate a transparent lens. All activities of the two kinds of cells were harmonious and did not cause opacity or shape deformity in the regenerated lens. Therefore, we can infer that D5 eEDCs may be composed of a mixture of cells. Meanwhile, we initially supposed to use exogenous eEDCs to supplement the seed cells of lens regeneration, it also caused some changes to the intraocular microenvironment, provided some new signals, and participated in some signal pathways related to lens transparency maintenance and continuous regeneration.

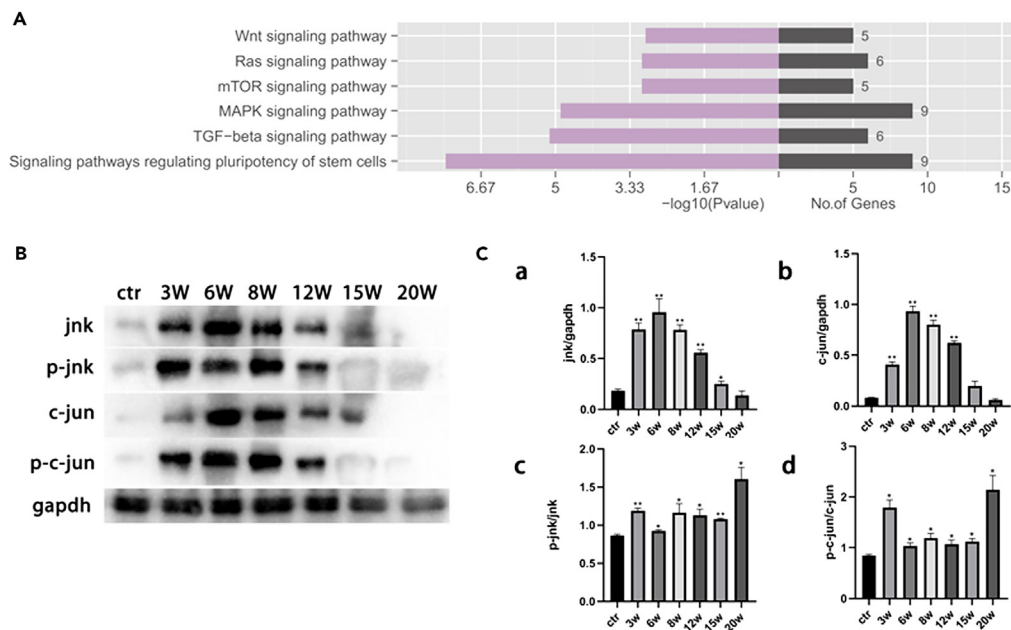


**Figure 8. Lens regeneration process is related to Wnt signaling pathway by stimulating JNK and c-JUN activity and their phosphorylation**

(A) KEGG pathway enrichment analysis indicated lens regeneration is associated with Wnt signaling pathway and its related pathways.

(B) Protein levels of JNK, p-JNK, c-JUN, and p-c-JUN measured by western blotting showed an increase in the lens regeneration process. GAPDH was used as an internal control.

(C) The changes of JNK, p-JNK, c-JUN, and p-c-JUN: (a) Total protein level of JNK showed an increase in the lens regeneration process.

(b) Total protein level of c-JUN showed an increase in the lens regeneration process.

(c) p-JNK protein levels relative to total JNK protein levels in the lens regeneration process were significantly higher than those in the control group.

(d) p-c-JUN protein levels relative to total c-JUN protein levels in the lens regeneration process were significantly higher than those in the control group. Data are expressed as the mean  $\pm$  standard deviation from three independent experiments. \* $p < 0.05$ , \*\* $p < 0.01$  vs. control; GAPDH, glyceraldehyde 3-phosphate dehydrogenase; ctr, control; JNK, c-JUN N-terminal kinase; p-JNK, phosphorylated c-JUN N-terminal kinase.

RNA sequencing and WB analysis after KEGG suggested that the occurrence of lens regeneration and the maintenance of transparency may be related to the synchronization and integration of the Wnt signaling pathway, which is a highly conservative signaling pathway in species evolution and widely exists in vertebrates and invertebrates. Wnt signaling plays an important role in early embryonic development, tissue regeneration, organ formation, and other physiological processes. However, the influence of Wnt on lens regeneration is still unknown. The Wnt signaling pathway is composed of canonical Wnt/ $\beta$ -catenin signaling and non-canonical Wnt signaling.<sup>16</sup> Aside from the classical Wnt/ $\beta$ -catenin pathway, at least two pathways are activated by Wnt ligands, and their effects are independent of  $\beta$ -catenin. These pathways, known as the non-canonical pathways, are grouped according to the Wnt receptor and co-receptors involved, as well as by the triggered intracellular signals—the PCP pathway and the Ca<sup>2+</sup> pathway. The Wnt/PCP pathway was first identified in *Drosophila* as regulating tissue polarity and cell migration during development.<sup>17</sup> As the Wnt/PCP pathway signals control cell polarity through c-Jun N-terminal kinase (JNK), it is thus also called the Wnt/JNK pathway.<sup>18,19</sup> In this pathway, the binding of Wnt to the Fz receptor on the membrane surface is followed by the activation of JNK. The downstream effect of this pathway is the regulation of the cytoskeletal organization, cell motility, and gene expression by JNK-dependent transcription factors, with concomitant activation of its target genes.<sup>20,21</sup>

Recent studies have emphasized the importance of the interaction between LECs and lens fibroblast cells.<sup>22</sup> It is well known that one of the key characteristics that distinguishes the lens fibroblast cells from the lens is that lens fibroblast cells are arranged in regular unidirectional strips under the

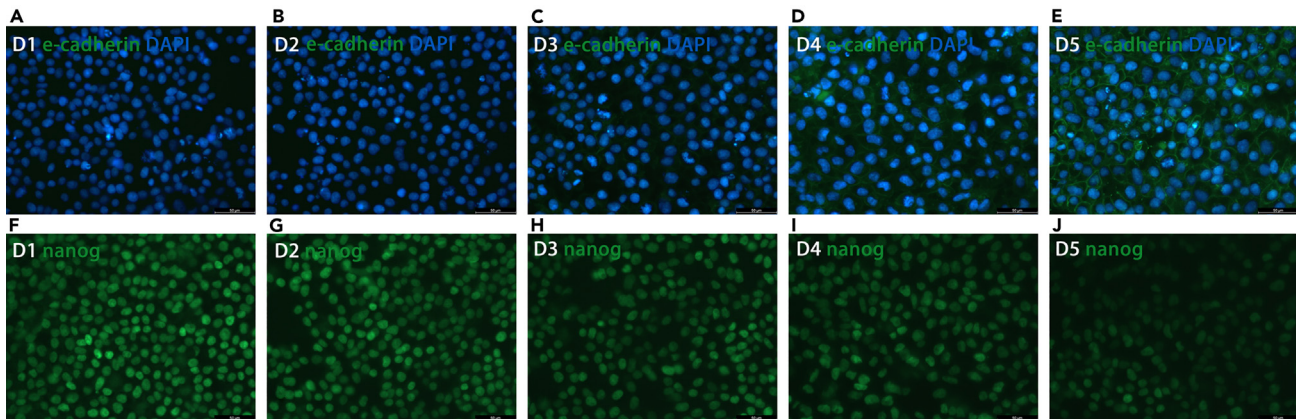


**Figure 9. Expression of epithelial cell marker E-cadherin (a–e, green) and stem cell marker Nanog (f–j, green) during the process of ESC differentiation *in vitro* by immunofluorescence (DAPI, blue)**

(A and B) E-cadherin, negative at D1 and D2.

(C and D) E-cadherin, little expression.

(E) E-cadherin, obvious expression at D5.

(F–I) Nanog expression slowly decreased.

(J) Nanog expression significantly decreased but still positive at D5.

single-layer LECs of the anterior capsule. Some studies have shown that the arrangement and polarization direction of lens fibroblast cells are related to the Wnt/PCP signal pathway.<sup>23</sup> At the same time, we found that under a certain stimulation control,<sup>24</sup> Wnt-related signals derived from LECs provided a kind of polarization clue, making the elongated fiber cells always aligned in the direction of the LECs, consistent with the orderly arrangement and polarization of the fibers.<sup>25,26</sup> This specific stimulation control may be related to the new environmental signal stimuli brought about by the implanted exogenous eEDCs described above.

It is well known that in the aqueous humor, a variety of cell growth factors are involved in the regulation of lens development, including fibroblast growth factor (FGF), epidermal growth factor (EGF), insulin-like growth factors (IGFs), and transforming growth factor B (TGF- $\beta$ ), among others,<sup>27</sup> which all act on different parts of the lens, affect the morphogenesis, proliferation, and differentiation of LECs and lens fibroblast cells, as well as guide the formation of lens polarity, thus affecting the development and transparency of the lens. For example, FGF is the only growth factor that can induce mammalian LECs to undergo many fiber-specific morphological and molecular changes, including elongation, structural specialization, and the initiation of specific crystallin expression. The binding of FGF to FGFR results in the autophosphorylation of FGFR and the activation of the downstream signaling pathway Wnt, MAPK, so as to participate in the process of cell proliferation, migration, and differentiation, as well as directly affect the development of the lens.<sup>28,29</sup> Furthermore, our RNA and KEGG pathway-enrichment analysis showed the involvement of these pathways, including Wnt and MAPK. FGF is considered to be the trigger factor in the differentiation of LECs into lens fibroblast cells during embryonic development, and it has a certain relationship with its concentration. The concentration gradient theory has been widely accepted, wherein low-dose FGF promotes cell proliferation, medium-concentration FGF promotes cell migration, and high-dose FGF induces differentiation.<sup>27,30</sup> However, lens transparency is related to cell proliferation, migration, and differentiation. Only the high-quality promotion of a certain cell activity cannot meet the requirements of uniform and transparent lens regeneration and maintenance. From the perspective of the postoperative process without any exogenous cell implantation, the changes of aqueous humor factors caused by external surgical stimulation can affect the proliferation, migration, and differentiation of lens fibroblast cells to a certain extent; however, the changes cannot achieve the appropriate microenvironment to support the coordination of the three cell activities.

Therefore, the exogenous eEDCs we implanted brought about new environmental stimuli to some extent; the Wnt/PCP pathway was activated during the whole process of lens regeneration, exhibiting a similar signal to that of lens development. Therefore, during the process of lens regeneration, lens fibroblast cells pass through the Wnt/PCP pathway under the regulation of Wnt-related signals, so as to achieve the

orderly growth and arrangement of lens fibroblast cells, as well as lens regeneration and transparency maintenance. Meanwhile, in the absence of any exogenous cell implantation, lens fibroblast cells have disorderly arrangement, and LECs have limited proliferation ability, leading to problems of thinness and the opacity of the regenerated lens. At the same time, we speculate that the regeneration depends only on the limited LECs arranged under the anterior capsule and at the equator, and the residual LECs may not be sufficient; thus, the regeneration ability is weak, and the thickness is insufficient.

The eEDCs we implanted were differentiated from hESCs at a very early stage of differentiation. These cells not only expressed epithelial markers but also maintained the characteristics of stem cells. Thus, we may deduce that the implanted eEDCs still had a high, strong proliferation ability. Moreover, we found that long after surgery, the process of lens regeneration continues. In addition, under the microenvironment of the lens capsule, the implanted cells not only migrate, differentiate, and proliferate with the endogenous LECs but also maintain a balance between the three cell activities of the two kinds of cells in the lens capsule. This means that the regenerated lens after the implantation of eEDCs is thicker and more transparent, which is consistent with our WB result that the proportion of human-derived cells in the total amount of lens at different regeneration times was almost constant. Therefore, we can infer that exogenous eEDCs and endogenous LECs have synergistic effects on lens regeneration.

Moreover, in the process of lens regeneration, we found that some areas of opacity and discordant regeneration became transparent and orderly after a period of time. We suppose that this may be because of the fact that the implanted stem cells continue to maintain the ability to self-renew and self-heal. In the future, more research could focus on this phenomenon; studying the mechanism of this process may open up a new chapter for the reversion of cataracts.

Sodium hyaluronate is a glycosaminoglycan found in various connective, epithelial, and neural tissues.<sup>31</sup> It has not been found to be toxic in a wide range of acute animal toxicity studies,<sup>32</sup> which have included several species and different exposure routes. In addition, sodium hyaluronate is not immunogenic, nor is it a sensitizer in animal studies; it is not a reproductive or developmental toxicant, and it is not genotoxic.<sup>33,34</sup> HA is widely used in ophthalmology as eye drops, which are viscous and viscoelastic substances. We chose HA as the carrier of implanted eEDCs inspired by the viscoelastic Healon<sup>R</sup> used in cataract surgery. Healon<sup>R</sup>, a 1% solution of highly purified HA, consists of very large hyaluronic acid chains with molecular weights between 2 and  $5 \times 10^6$  and has a viscosity as high as 100 to  $300 \times 10^3$  cSt.<sup>35</sup> One of its great advantages is that the transition from viscous to elastic behavior occurs at low concentrations and low velocities. Owing to its elasticity, Healon<sup>R</sup> can be injected easily through a 30-gauge cannula but still retain its original shape in aqueous low velocities. The main disadvantage of using viscoelastic is the significant elevation of intraocular pressure seen postoperatively if any is retained (not completely removed during surgery). It is presumed that this is the result of large molecules of viscoelastic creating mechanical resistance in the trabecular meshwork. In addition, we carried out numerous pre-experiments on HA concentration and molecular weight to obtain the appropriate concentration and molecular weight for the current study. We hoped to obtain an HA both viscous and elastic and that can fix the target eEDCs to attach to the capsule, but its molecular weight too large to block the trabecular meshwork, and can completely metabolize from aqueous humor and the capsule within one week. Therefore, we chose HA with a molecular weight of  $1.5 \times 10^6$  and a concentration of 1.5% as the final carrier material, because it met all the requirements outlined above. At the same time, according to the results of slit lamp examination and post-operative IOP detection, the current HA did not block the trabecular meshwork. The IOP increased slightly on the first day after surgery and returned to normal levels on the third day after surgery. No obvious HA residue was observed on the third day after surgery. Therefore, the existence of HA can be considered not to pose a threat to the safety of rabbit eyes.

In this study, we used exogenous eEDCs mixed with HA gel to implant into the lens capsule, successfully achieving lens regeneration. The regenerated lens expressed mature lens markers. Furthermore, WB and RNA sequencing were used to verify that part of the regenerated lens was derived from the implanted cells. At the same time, the safety evaluation showed that the experimental method did not cause damage to the rabbit eyes. The regenerated lens in this study was not perfect, but it was the most transparent, thickest, and most similar to the original natural lens that has been reported in the literature thus far. This provides a new therapeutic strategy and development direction for cataracts, beginning a new era for the diagnosis and treatment of cataract and other lens diseases.

## LIMITATIONS OF STUDY

Although the regenerated lens reported in this study is the most transparent, thickest, and most similar to the original natural lens in shape and refractive diopter; however, the regenerated lens is not perfect, there is still a long way to go to clinical applications. Besides, we used eEDCs implanted into the rabbit lens capsule to successfully regenerate the lens, the eEDCs may be a mixture of cells at various induction stage and with different fate, we still have no way to figure out the most effective cells or cell combinations that play a decisive role in this regeneration process. Although completing this research, we will conduct the next step of research, starting from the phenomenon of lens regeneration to conduct mechanism and molecular biology research, so that the process of lens regeneration can be improved from the mechanism, so as to achieve the goal of regenerating a lens that is completely the same as the natural lens.

## STAR★METHODS

Detailed methods are provided in the online version of this paper and include the following:

- KEY RESOURCES TABLE
- RESOURCE AVAILABILITY
  - Lead contact
  - Materials availability
  - Data and code availability
- EXPERIMENTAL MODEL AND SUBJECT DETAILS
  - Rabbits
- METHOD DETAILS
  - Cell culture and differentiation
  - Carrier material preparation and cell mix
  - Surgical technique
  - Clinical evaluation
  - Histological analysis
  - Immunofluorescence
  - Western blot analysis
  - Immunofluorescence and immunohistochemistry
  - RNA sequencing analysis
  - Calcein AM/PI staining
  - Tumorigenicity experiment
- QUANTIFICATION AND STATISTICAL ANALYSIS

## SUPPLEMENTAL INFORMATION

Supplemental information can be found online at <https://doi.org/10.1016/j.isci.2023.106921>.

## ACKNOWLEDGMENTS

We would like to thank Weifeng Ma and other colleagues from the Zhejiang Academy of Medical Sciences for your help in raising and taking care of experimental animals. Dr. Ke Yao was funded by Program of National Natural Science Foundation of China (81870641), Program of National Natural Science Foundation of China (82070939) and Zhejiang Province Key Research and Development Program (2020C03035). Dr. Xinyi Chen was funded by Medical Health Science and Technology Project of Zhejiang Provincial Health Commission (2022RC031) and Zhejiang Provincial Natural Science Foundation of China (LQ23H120005).

## AUTHOR CONTRIBUTIONS

Conceptualization: X.C., Q.F., and K.Y.; Methodology: X.C., H.W., H.C., L.R., and W.W.; Investigation: X.C., H.W., H.C., L.R., and P.H.; Analysis: X.C., H.W., H.C., and J.X.; Writing—original draft: X.C. and H.W.; Writing—review and editing: H.C., L.R., W.W., J.X., C.L., Q.F., and K.Y.; Supervision: Q.F. and K.Y.

## DECLARATION OF INTERESTS

The authors declare no competing interests.

Received: June 29, 2022

Revised: March 6, 2023

Accepted: May 15, 2023

Published: May 19, 2023

## REFERENCES

- SeeInternational. Cataracts. <https://www.seeintl.org/cataracts/>.
- NEI. Cataract data and statistics. <https://www.nei.nih.gov/learn-about-eye-health/resources-for-health-educators/eye-health-data-and-statistics/cataract-data-and-statistics>.
- Chen, X., Xu, J., Chen, X., and Yao, K. (2021). Cataract: advances in surgery and whether surgery remains the only treatment in future. *Advances in Ophthalmology Practice and Research* 1, 100008. <https://doi.org/10.1016/j.aopr.2021.100008>.
- Vergara, M.N., Tsissios, G., and Del Rio-Tsonis, K. (2018). Lens regeneration: a historical perspective. *Int. J. Dev. Biol.* 62, 351–361. <https://doi.org/10.1387/ijdb.180084nv>.
- Gu, Y., Yao, K., and Fu, Q. (2021). Lens regeneration: scientific discoveries and clinical possibilities. *Mol. Biol. Rep.* 48, 4911–4923. <https://doi.org/10.1007/s11033-021-06489-5>.
- Henry, J.J., and Hamilton, P.W. (2018). Diverse evolutionary origins and mechanisms of lens regeneration. *Mol. Biol. Evol.* 35, 1563–1575. <https://doi.org/10.1093/molbev/msy045>.
- Gwon, A. (2006). Lens regeneration in mammals: a review. *Surv. Ophthalmol.* 51, 51–62. <https://doi.org/10.1016/j.survophthal.2005.11.005>.
- Lin, H., Ouyang, H., Zhu, J., Huang, S., Liu, Z., Chen, S., Cao, G., Li, G., Signer, R.A.J., Xu, Y., et al. (2016). Lens regeneration using endogenous stem cells with gain of visual function. *Nature* 531, 323–328. <https://doi.org/10.1038/nature17181>.
- Placantonakis, D.G., Tomishima, M.J., Lafaille, F., Desbordes, S.C., Jia, F., Socci, N.D., Viale, A., Lee, H., Harrison, N., Tabar, V., and Studer, L. (2009). BAC transgenesis in human embryonic stem cells as a novel tool to define the human neural lineage. *Stem Cell.* 27, 521–532. <https://doi.org/10.1634/stemcells.2008-0884>.
- Liu, Z., Wang, R., Lin, H., and Liu, Y. (2020). Lens regeneration in humans: using regenerative potential for tissue repairing. *Ann. Transl. Med.* 8, 1544. <https://doi.org/10.21037/atm-2019-rscs-03>.
- Wu, W., Lois, N., Prescott, A.R., Brown, A.P., Van Gerwen, V., Tassignon, M.J., Richards, S.A., Saunter, C.D., Jarrin, M., and Quinlan, R.A. (2021). The importance of the epithelial fibre cell interface to lens regeneration in an in vivo rat model and in a human bag-in-the-lens (BiL) sample. *Exp. Eye Res.* 213, 108808. <https://doi.org/10.1016/j.exer.2021.108808>.
- Vavvas, D.G., Dryja, T.P., Wilson, M.E., Olsen, T.W., Shah, A., Jurkunas, U., Pineda, R., Poulaki, V., Palioura, S., Veldman, P., et al. (2018). Lens regeneration in children. *Nature* 556, E2–E3. <https://doi.org/10.1038/nature26149>.
- Ooto, S., Haruta, M., Honda, Y., Kawasaki, H., Sasai, Y., and Takahashi, M. (2003). Induction of the differentiation of lentoids from primate embryonic stem cells. *Invest. Ophthalmol. Vis. Sci.* 44, 2689–2693. <https://doi.org/10.1167/iovs.02-1168>.
- Yang, C., Yang, Y., Brennan, L., Bouhassira, E.E., Kantorow, M., and Cvekl, A. (2010). Efficient generation of lens progenitor cells and lentoid bodies from human embryonic stem cells in chemically defined conditions. *Faseb. J.* 24, 3274–3283. <https://doi.org/10.1096/fj.10-157255>.
- Fu, Q., Qin, Z., Jin, X., Zhang, L., Chen, Z., He, J., Ji, J., and Yao, K. (2017). Generation of functional lentoid bodies from human induced pluripotent stem cells derived from urinary cells. *Invest. Ophthalmol. Vis. Sci.* 58, 517–527. <https://doi.org/10.1167/iovs.16-20504>.
- Xiang, T., Li, L., Yin, X., Zhong, L., Peng, W., Qiu, Z., Ren, G., and Tao, Q. (2013). Epigenetic silencing of the WNT antagonist Dickkopf 3 disrupts normal Wnt/beta-catenin signalling and apoptosis regulation in breast cancer cells. *J. Cell Mol. Med.* 17, 1236–1246. <https://doi.org/10.1111/jcmm.12099>.
- Adler, P.N. (2002). Planar signaling and morphogenesis in *Drosophila*. *Dev. Cell* 2, 525–535. [https://doi.org/10.1016/s1534-5807\(02\)00176-4](https://doi.org/10.1016/s1534-5807(02)00176-4).
- Boutros, M., Paricio, N., Strutt, D.I., and Mlodzik, M. (1998). Dishevelled activates JNK and discriminates between JNK pathways in planar polarity and wingless signaling. *Cell* 94, 109–118. [https://doi.org/10.1016/s0092-8674\(00\)81226-x](https://doi.org/10.1016/s0092-8674(00)81226-x).
- Yamanaka, H., Moriguchi, T., Masuyama, N., Kusakabe, M., Hanafusa, H., Takada, R., Takada, S., and Nishida, E. (2002). JNK functions in the non-canonical Wnt pathway to regulate convergent extension movements in vertebrates. *EMBO Rep.* 3, 69–75. <https://doi.org/10.1093/embo-reports/kvf008>.
- Simons, M., and Mlodzik, M. (2008). Planar cell polarity signaling: from fly development to human disease. *Annu. Rev. Genet.* 42, 517–540. <https://doi.org/10.1146/annurev.genet.42.110807.091432>.
- Kikuchi, A., Yamamoto, H., Sato, A., and Matsumoto, S. (2011). New insights into the mechanism of Wnt signaling pathway activation. *Int. Rev. Cell Mol. Biol.* 291, 21–71. <https://doi.org/10.1016/B978-0-12-386035-4.00002-1>.
- McAvoy, J.W., Dawes, L.J., Sugiyama, Y., and Lovicu, F.J. (2017). Intrinsic and extrinsic regulatory mechanisms are required to form and maintain a lens of the correct size and shape. *Exp. Eye Res.* 156, 34–40. <https://doi.org/10.1016/j.exer.2016.04.009>.
- Sugiyama, Y., Lovicu, F.J., and McAvoy, J.W. (2011). Planar cell polarity in the mammalian eye lens. *Organogenesis* 7, 191–201. <https://doi.org/10.4161/org.7.3.18421>.
- Dawes, L.J., Sugiyama, Y., Tanedo, A.S., Lovicu, F.J., and McAvoy, J.W. (2013). Wnt-frizzled signaling is part of an FGF-induced cascade that promotes lens fiber differentiation. *Invest. Ophthalmol. Vis. Sci.* 54, 1582–1590. <https://doi.org/10.1167/iovs.12-11357>.
- Dawes, L.J., Sugiyama, Y., Lovicu, F.J., Harris, C.G., Shelley, E.J., and McAvoy, J.W. (2014). Interactions between lens epithelial and fiber cells reveal an intrinsic self-assembly mechanism. *Dev. Biol.* 385, 291–303. <https://doi.org/10.1016/j.ydbio.2013.10.030>.
- Sugiyama, Y., Stump, R.J.W., Nguyen, A., Wen, L., Chen, Y., Wang, Y., Murdoch, J.N., Lovicu, F.J., and McAvoy, J.W. (2010). Secreted frizzled-related protein disrupts PCP in eye lens fiber cells that have polarised primary cilia. *Dev. Biol.* 338, 193–201. <https://doi.org/10.1016/j.ydbio.2009.11.033>.
- Lovicu, F.J., and McAvoy, J.W. (2005). Growth factor regulation of lens development. *Dev. Biol.* 280, 1–14. <https://doi.org/10.1016/j.ydbio.2005.01.020>.
- Henry, J.J., Thomas, A.G., Hamilton, P.W., Moore, L., and Perry, K.J. (2013). Cell signaling pathways in vertebrate lens regeneration. *Curr. Top. Microbiol. Immunol.* 367, 75–98. [https://doi.org/10.1007/82\\_2012\\_289](https://doi.org/10.1007/82_2012_289).
- Sakamoto, M., Morimoto, N., Ogino, S., Jinno, C., Taira, T., and Suzuki, S. (2016). Efficacy of gelatin gel sheets in sustaining the release of basic fibroblast growth factor for murine skin defects. *J. Surg. Res.* 201, 378–387. <https://doi.org/10.1016/j.jss.2015.11.045>.
- McAvoy, J.W., and Chamberlain, C.G. (1989). Fibroblast growth factor (FGF) induces different responses in lens epithelial cells depending on its concentration. *Development* 107, 221–228. <https://doi.org/10.1242/dev.107.2.221>.
- Viswanathan, S., Adibi, A., and Bhatt, S. (2017). MSCs translational process. In *Mesenchymal Stromal Cells* (Elsevier), pp. 1–35.
- Schauss, A.G., Merkel, D.J., Glaza, S.M., and Sorenson, S.R. (2007). Acute and subchronic oral toxicity studies in rats of a hydrolyzed chicken sternal cartilage preparation. *Food*

- Chem. Toxicol. 45, 315–321. <https://doi.org/10.1016/j.fct.2006.08.011>.
33. Bagchi, M., Patel, S., Zafra-Stone, S., and Bagchi, D. (2011). Selected herbal supplements and nutraceuticals. In *Reproductive and Developmental Toxicology* (Elsevier), pp. 385–393.
34. Becker, L.C., Bergfeld, W.F., Belsito, D.V., Klaassen, C.D., Marks, J.G., Jr., Shank, R.C., Slaga, T.J., Snyder, P.W.; Cosmetic Ingredient Review Expert Panel, and Andersen, F.A. (2009). Final report of the safety assessment of hyaluronic acid, potassium hyaluronate, and sodium hyaluronate. *Int. J. Toxicol.* 28, 5–67. <https://doi.org/10.1177/1091581809337738>.
35. Eisner, G. (1985). The use of viscous and viscoelastic substances in ophthalmology. In *Recent Advances in Ophthalmology* (Elsevier), pp. 31–62.

## STAR★METHODS

### KEY RESOURCES TABLE

REAGENT or RESOURCE	SOURCE	IDENTIFIER
<b>Antibodies</b>		
mouse anti-FOXE3	Santa Cruz	sc-377465
rabbit anti- $\beta$ -crystallin	Santa Cruz	sc-22745
mouse anti- $\gamma$ -crystallin	Santa Cruz	sc-365256
mouse anti- $\alpha$ B-crystallin	Enzo	ADI-SPP-225-L
mouse anti- $\alpha$ A-crystallin	Enzo	ADI-SPP-225-L
rabbit anti-GAPDH	Cell signaling	92310
<b>Experimental models: Cell lines</b>		
Human: HUES 9 hESC line	Cell Bank	N/A
<b>Experimental models: Organisms/strains</b>		
New Zealand Rabbit	Kelian Rabbit Industry Professional Cooperative	N/A
<b>Software and algorithms</b>		
Statistical Package for the Social Sciences	IBM	<a href="https://www.ibm.com/analytics/spss-statistics-software">https://www.ibm.com/analytics/spss-statistics-software</a>

### RESOURCE AVAILABILITY

#### Lead contact

Further information and requests for resources and reagents should be directed to and will be fulfilled by the lead contact, Ke Yao ([xlren@zju.edu.cn](mailto:xlren@zju.edu.cn)).

#### Materials availability

This study did not generate new unique reagents.

#### Data and code availability

- All data reported in this paper will be shared by the [lead contact](#) upon request.
- This paper does not report original code.
- Any additional information required to reanalyze the data reported in this paper is available from the [lead contact](#) upon request.

### EXPERIMENTAL MODEL AND SUBJECT DETAILS

#### Rabbits

This experiment selected 6-month-old female New Zealand rabbits (weighing 2-2.5kg), purchased from Hangzhou Yuhang Kelian Rabbit Industry Professional Cooperative. New Zealand rabbits were all raised in single cages, and the breeding environment complied with the national standard "Experimental Animal Environment and Facilities" (GB 14925-2010). Provide sufficient feed and clean water sources for single cage New Zealand rabbits, maintain an ambient temperature of 15-25°C and air humidity of 60-70% in the animal room, and disinfection and pest prevention work were regularly carried out. All experimental rabbits were given adaptive feeding for one week before receiving the experiment. All animal experiments were approved by the Institutional Animal Care and Use Committee of Zhejiang University.

Forty female New Zealand white rabbits were divided into eight groups, with five rabbits per euthanized group (Group A: 3 weeks [W]; Group B: 6 W; Group C: 8 W; Group D: 11 W; Group E: 15 W; Group F: 20 W), five for long-term observation until normal death (Group G), and five for surgery without cell implantation (Group H). (Four rabbits died from systemic infections unrelated to surgery. The remaining 36 rabbits

were used to assess regeneration). The rabbits were raised individually in cages under standard breeding conditions.

## METHOD DETAILS

### Cell culture and differentiation

H9 human ESCs (Cell Bank, Shanghai, China) were cultured in mTesR medium (Stemcell, BC, Canada) in a six-well dish (Costar, Corning Life Sciences) coated with Matrigel (BD Biosciences, Bedford, MA, USA) and differentiated to a lens fate using the protocol described in a previous study in detail (Fu et al., 2017). The ESCs were 1:8 passaged at D0 with 0.5 mM EDTA in phosphate-buffered saline (PBS). One day after plating, the ESCs were triggered via 100 ng/ml of the bone morphogenetic protein (BMP) inhibitor noggin, and the concentration of the noggin (R&D Systems, MN, USA) was maintained for differentiation until D5 to obtain eEDCs. Additionally, the culture medium was changed every day.

### Carrier material preparation and cell mix

Sodium hyaluronate (15 mg) (HA; Bloomage Freda Biopharm Co., Ltd., Jinan, China) powder was dissolved in 0.5 ml of mTesR medium to obtain 3% HA-mTesR gel in a 1.5-ml tube. The eEDCs were collected at D5, 0.5 mM of EDTA was added for dissociation, and then 0.5 ml of mTesR was added to detach the cells from the culture plates; 0.5 ml of the dissociated cells were transferred and mixed with the 0.5 ml of HA-mTesR gel to obtain 1 ml of the eEDCs-HA gel compound.

### Surgical technique

Before surgery, atropine sulfate ophthalmic gel (Shenyang Sinqi Pharmaceutical Co., Ltd., China) was applied four times daily for one day, and tropicamide (Santen Pharmaceutical Co., Ltd., Japan) was given every 15 minutes (three times) for pupil dilation. Sodium pentobarbital saline solution (3.0 mg/100 mL) was administered intravenously for surgical-depth anesthesia. A 3.0-mm single-plane main incision and an 0.8-mm side-port corneal incision were made with a keratome. To achieve uniformly capsulorhexis, we established a new micro-capsulotomy, which improved on the base of the previous study (Lin et al., 2016). We used a 30-degree-tip phaco handpiece (DP8230, Bausch & Lomb, Inc.) without an irrigation tube to punch a 0.9-mm capsulotomy peripherally at 11 o'clock (Figure S1A). Next, phacoemulsification and I/A were used to remove the cortex of the primary lens. We extracted eEDCs-HA gel using a 1-ml syringe without a needle, doing so slowly to prevent air bubbles, and then injected 0.2 ml of eEDCs-HA gel through the 0.9-mm capsulorhexis using irrigation needles (Shanghai Kindly Enterprises Development Group Co., Ltd., China) (Figure S1C). Finally, the limbus wound was sutured with an interrupted 10-0 nylon suture. After surgery, topical dexamethasone tobramycin (Alcon, TX, USA) was applied four times a day for two weeks and pranopfen (Senju Pharmaceutical Co., Ltd., Japan) was administered for one month to the operated eye.

### Clinical evaluation

Comprehensive clinical evaluations were performed. We examined anterior chamber conditions and lens regeneration via slit lamp (BQ 900, Haag-Streit AG) at D1, D3, and D7 every week from the second week, and every two weeks from 54W. IOP was obtained using the Reichert Tonopen XL Tonometer (Veatch Ophthalmic Instruments, AZ, USA) at D1, D3, D7, W2, and W4. Pentacam (Oculus Optikgeräte GmbH) and ultrasound biomicroscopy (UBM) (SUOER UBMScan SW-3200) were used to obtain lens regeneration morphology *in vivo* before 12 W and at 54 W. In terms of the limitation of these two instruments regarding depth, they could not be used routinely after 12 W. The diopter of both eyes was determined by retinoscopy, which was performed by an experienced optometrist. Measurement was performed approximately 45 min after cycloplegia was induced by tropicamide every 15 min (three times). Rabbits were euthanized at 3, 6, 8, 12, 15, and 20 W after surgery, and the treated eyes were enucleated. All rabbits were subjected to a general and basic eye examination to confirm their health status before being sacrificed; moreover, their body weight was recorded before being euthanized. The lenses were harvested for histologic and western blot (WB) analysis.

### Histological analysis

A human lens was obtained from a 20-year-old male whose organs were donated upon his accidental death. The human lens and regenerated lens specimens were fixed in 4% paraformaldehyde, dehydrated through a series of graded ethanol, embedded in paraffin, and then cut into 5- $\mu$ m-thick sections. For histological observation, the sections were stained with hematoxylin and eosin (H&E).

### Immunofluorescence

For immunofluorescence examination, slides were prepared in the same way as for H&E staining—paraffin sections of the lens specimens were rehydrated and boiled in ethylenediaminetetraacetic acid buffer for 10 min to induce antigen retrieval. After blocking for 1 h at room temperature with blocking solution (20% bovine serum albumin and 0.5% tritonX-100 [Sigma–Aldrich]), the sections were incubated overnight with the following primary antibodies: mouse anti-FOXE3 (1:200) (Santa Cruz), rabbit anti- $\beta$ -crystallin (1:200) (Santa Cruz), mouse anti- $\gamma$ -crystallin (1:200) (Santa Cruz), mouse anti- $\alpha$ B-crystallin (1:100) (Enzo), and mouse anti- $\alpha$ A-crystallin (1:100) (Enzo). Subsequently, the lenses were incubated for 1.5 h with AlexaFluor-555–labeled secondary antibody (1/1000) (Invitrogen), and the nuclei were labeled with 4',6-diamidino-2-phenylindole (DAPI) (0.5  $\mu$ g/ml; Sigma–Aldrich). Finally, images were captured using an Olympus IX71 microscope that was equipped with DP2-BSW software (Olympus) and prepared using ImageJ software and Microsoft PowerPoint (2007).

### Western blot analysis

The regeneration lens samples at 3, 6, 8, 12, 15, and 20 W, untreated rabbit lenses, and human ESCs were lysed with extraction buffer (Sangon Biotech Co., Ltd., China). Human lens protein was collected from patients undergoing phacoemulsification. The protein concentration was then determined using a BCA Protein Assay Kit (Thermo Fisher Scientific, USA) as well as a spectrophotometer (Bio-Rad iMark Microplate Reader). From each sample, 20- $\mu$ g extracts were loaded into the designated lanes. All proteins were separated and transferred onto a PVDF blotting membrane. The membranes with the targeted proteins were then incubated overnight with rabbit anti- $\gamma$ -crystalline (Cell signaling) and rabbit anti-GAPDH (Cell signaling) primary antibody at a 1:1000 dilution. After incubation with a horseradish peroxidase (HRP)–conjugated second antibody (cell signaling) (1:5000), the images were developed using the ECL detection system (Millipore) and the ChemiDoc™ MP imaging system (Bio-Rad).

### Immunofluorescence and immunohistochemistry

Slides were prepared in the same way as for H&E staining—paraffin sections of the lens specimens were rehydrated and boiled in ethylenediaminetetraacetic acid buffer for 10 min to induce antigen retrieval. After blocking for 1 h at room temperature with the blocking solution (20% bovine serum albumin and 0.5% tritonX-100 [Sigma–Aldrich]), human ESCs were treated with noggin and fixed in 4% paraformaldehyde from D1 to D5. The sections and cells were incubated overnight with the following primary antibodies: mouse anti-FOXE3 (1:200) (Santa Cruz), rabbit anti- $\beta$ -crystallin (1:200) (Santa Cruz), mouse anti- $\gamma$ -crystallin (1:200) (Santa Cruz), mouse anti- $\alpha$ B-crystallin (1:100) (Enzo), mouse anti- $\alpha$ A-crystallin (1:100) (Enzo), mouse anti-e-cadherin (1:500) (cell signaling), and mouse anti-Nanog (1:500) (Santa Cruz) for cell immunofluorescence; and rabbit anti-GAPDH (1:400) (cell signaling) for immunohistochemistry. Subsequently, the slides and cells were incubated for 1.5 h with AlexaFluor-555–labeled secondary antibody (1:1000) (Invitrogen) and HRP-conjugated second antibody (1:1000) (cell signaling). For immunofluorescence examination, the nuclei were labeled with 4',6-diamidino-2-phenylindole (DAPI) (0.5  $\mu$ g/ml; Sigma–Aldrich), and images were captured using a Leica DMI8 microscope (Leica). For immunohistochemistry, slides were stained using a DAB kit (ZSGB-Bio, China), and the nuclei were stained with hematoxylin.

### RNA sequencing analysis

Total RNA was extracted from the regeneration lens using TRIzol (Life Technologies, USA) according to the manufacturer's protocol. RNA purity was assessed using the ND-2000c Nanodrop (Thermo Fisher Scientific). Each RNA sample had an A260:A280 ratio between 1.8 and 2.0. RNA integrity was evaluated using the Agilent 2200 TapeStation (Agilent Technologies, USA), and each sample had an RIN above 7.0. The rRNAs were removed from the total RNA and fragmented to approximately 200 bp. The purified RNAs were subjected to first- and second-strand cDNA synthesis following adaptor ligation and enrichment using a low cycle according to the instructions of the NEBNext Ultra RNA Library Prep Kit for Illumina (NEB, USA). Subsequently, the purified library products were evaluated using the Agilent 2200 TapeStation and Qubit 2.0 (Life Technologies, USA) and then diluted to 10 pM for cluster generation *in situ* on the pair-end flow cell, followed by sequencing (2x150bp) using HiSeq3000.

Paired-end reads were aligned with the rabbit reference genome with HISAT2. Excluding gene matching with the rabbit, the rest gene reads were aligned with the human reference genome. HTSeq v.0.6.0 was used to count the number of readmapped to each gene, and the ratio of reads mapped to each reference

genome was calculated. Differently expressed genes were chosen according to the criteria of a fold change >2 and an adjusted p-value <0.05. All the differentially expressed genes were used for heatmap analysis and KEGG ontology enrichment analysis.

### Calcein AM/PI staining

Human ESCs were cultured in HA-mTesR gel for five days. The medium was changed every day. Each day, from D1 to D5, the cells were analyzed with Calcein AM (1:1000) (Invitrogen) and propidium iodide (PI) (1:1000) (Invitrogen) staining for 0.5 h in a cell incubator at 37°C. Fluorescence was observed using a Leica DMI8 microscope (Leica).

### Tumorigenicity experiment

Twenty healthy male athymic BALB/c (nu/nu) nude mice were purchased from Shanghai Jihui Laboratory Animal Care Co., Ltd. (Shanghai, China). The mice were six weeksold and each weighed 18–20 g. The mice were housed and fed in a specific pathogen-free (SPF) environment and provided with sterile food and water. All procedures were performed under aseptic conditions.  $3 \times 10^6$  HCCML-3 cells were washed with 100  $\mu$ L of PBS, eEDCs washed with 100  $\mu$ L of PBS, eEDCs with 100  $\mu$ L of Matrigel cell suspension, 100  $\mu$ L of normal saline (NS) were injected into subcutaneous tissue of five nude mice, using a 1-mL syringe with a 26-G needle. The animals were monitored for four weeks. At the end of the experiments, the mice were sacrificed, and the tumors were removed and observed.

### QUANTIFICATION AND STATISTICAL ANALYSIS

Continuous variables were expressed as mean  $\pm$  SD. The paired t-test was used to compare the intraocular pressure (IOP) and diopters between the operated eyes and contralateral eyes. Repeated-measures analysis of variance and multiple comparison tests were used to compare the IOP in the operated eyes at different timepoints. A P-value less than 0.05 was considered statistically significant. An unpaired t-test was used in the comparison of human reference genome–matching rates. All analyses (except when noted) were performed using the Statistical Package for the Social Sciences (SPSS) software (version 22.0, International Business Machines Corp.).